

# Singlet–Singlet Energy Transfer Mechanisms in Covalently-Linked Fucoxanthin– and Zeaxanthin–Pyropheophorbide Molecules

Martin P. Debreczeny,<sup>†</sup> Michael R. Wasielewski,<sup>\*,†,‡</sup> Satoshi Shinoda,<sup>§</sup> and Atsuhiko Osuka<sup>\*,§</sup>

Contribution from the Chemistry Division, Argonne National Laboratory, Argonne, Illinois 60439-4831, Department of Chemistry, Northwestern University, Evanston, Illinois 60208-3113, and Department of Chemistry, Faculty of Science, Kyoto University, Kyoto 606-01, Japan

Received February 24, 1997<sup>⊗</sup>

**Abstract:** Two carotenoids, fucoxanthin and zeaxanthin, were covalently attached to each of five different pyropheophorbides. Singlet–singlet energy transfer within these ten carotenopyropheophorbide compounds was measured by femtosecond transient absorption spectroscopy and steady-state fluorescence excitation spectroscopy. In all five compounds containing fucoxanthin, energy transfer was found to occur from the higher-lying fucoxanthin S<sub>1</sub> state to the lower-lying pyropheophorbide S<sub>1</sub> state with 12–44% efficiency. The multiple saturated bonds separating the  $\pi$  systems of the fucoxanthin and pyropheophorbide molecules, the fact that the fucoxanthin S<sub>1</sub>  $\leftrightarrow$  S<sub>0</sub> transition is partially allowed, and the good agreement between experimental and calculated energy transfer rates suggest that the Coulomb (Förster) mechanism is more important than the electron exchange (Dexter) mechanism for singlet–singlet energy transfer in these compounds. In contrast, all five zeaxanthin-containing compounds showed no clear evidence of energy transfer from the zeaxanthin S<sub>1</sub> state to the pyropheophorbide S<sub>1</sub> state. This is consistent with placing the zeaxanthin S<sub>1</sub> state energy level slightly below that of all the pyropheophorbides examined here. However, energy transfer efficiencies of up to 15% were observed from the zeaxanthin S<sub>2</sub> state to the pyropheophorbide S<sub>1</sub> state. These results suggest that several energy transfer mechanisms may operate simultaneously when carotenoid–chlorophyll distances are short.

## Introduction

Despite their short singlet excited-state lifetimes, carotenoids harvest light with high efficiency in photosynthetic organisms that are exposed to low-light conditions.<sup>1,2</sup> Absorbing light in the 450–550-nm region where chlorophyll absorption is weak, carotenoids can undergo rapid singlet–singlet excited-state energy transfer to chlorophyll. In contrast, under conditions of high light intensity, carotenoids can dissipate excess energy through singlet energy transfer from chlorophyll to carotenoid and/or fulfill a photoprotective role by quenching chlorophyll triplet states.

How carotenoids can play such diverse roles in the same organism has been the subject of numerous investigations. For example, the xanthophyll cycle, in which violaxanthin, antheraxanthin, and zeaxanthin are interconverted by epoxidation/de-epoxidation, plays an important role in light regulation in higher plants and green algae.<sup>3–5</sup> Epoxidation/de-epoxidation changes the conjugation length of these carotenoids, resulting in large changes in their lowest excited singlet state lifetimes and energy levels.<sup>1</sup> To promote efficient light harvesting the carotenoid

singlet energy donor should have a long singlet excited-state lifetime, as well as a singlet excited-state energy that is above that of the chlorophyll energy acceptor. De-epoxidation results in lengthening of the conjugation path of the carotenoid, resulting in a lower excited singlet state energy and a shorter singlet state lifetime, thereby reducing energy transfer efficiency to the chlorophyll.

Despite extensive characterization of carotenoids within photosynthetic organisms, the detailed mechanism by which energy is transferred to chlorophylls remains unclear. Among the many factors contributing to the difficulty in understanding carotenoid energy transfer are the following: (a) the experimental difficulty involved in determining the lowest excited singlet state energy levels in carotenoids, (b) the rapid time scale on which energy transfer occurs, (c) the difficulty in extracting rate constants for energy transfer between individual chromophore pairs within large arrays of chromophores, and (d) the paucity of structural information on photosynthetic light-harvesting antennas that contain carotenoids.<sup>6</sup>

The uncertainties in the energies of the lowest excited singlet states of carotenoids stem from the fact that the electronic transition from the ground state (S<sub>0</sub>) to the first excited singlet state (S<sub>1</sub>) in many carotenoids is either symmetry forbidden and/or masked by the greater oscillator strength of the S<sub>0</sub> state to second excited singlet state (S<sub>2</sub>) transition. Decay from S<sub>2</sub> to S<sub>1</sub> occurs on a 100 fs time scale, while decay from S<sub>1</sub> to S<sub>0</sub>

\* Address correspondence to these authors.

<sup>†</sup> Argonne National Laboratory.

<sup>‡</sup> Northwestern University.

<sup>§</sup> Kyoto University.

<sup>⊗</sup> Abstract published in *Advance ACS Abstracts*, June 15, 1997.

(1) Frank, H. A.; Cogdell, R. J. *Photochem. Photobiol.* **1996**, *63*, 257.

(2) Koyama, Y.; Kuki, M.; Andersson, P. O.; Gillbro, T. *Photochem. Photobiol.* **1996**, *63*, 243.

(3) Gilmore, A. M.; Yamamoto, H. Y. *Proc. Natl. Acad. Sci. U.S.A.* **1992**, *89*, 1899.

(4) Horton, P.; Ruban, A. V. *Photosynth. Res.* **1992**, *34*, 375.

(5) Demmig, B.; Winter, K.; Kruger, A.; Czygan, F.-C. *Plant Physiol.* **1987**, *84*, 218.

(6) Crystal structures have been determined for the B800-850 light-harvesting complex in a purple bacterium and the light-harvesting complex associated with photosystem II in green plants and algae (Mcdermott, G.; Prince, S. M.; Freer, A. A.; Hawthornthwaite-Lawless, A. M.; Papiz, M. Z.; Cogdell, R. J.; Isaacs, N. W. *Nature* **1995**, *374*, 517. Kühlbrandt, W.; Wang, D. N.; Fujiyoshi, Y. *Nature* **1994**, *367*, 614).

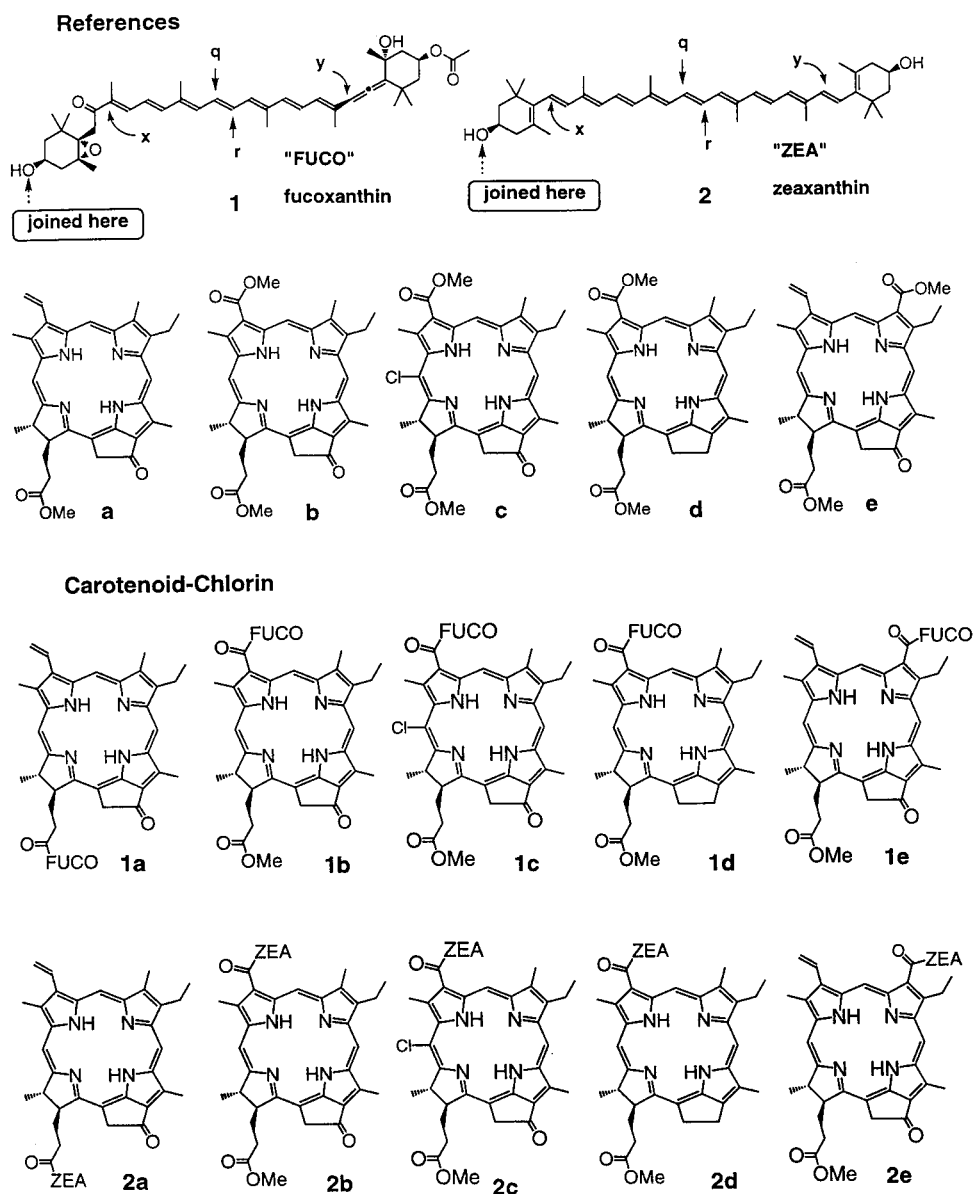


**Figure 1.** Structures of the molecules.

generally occurs on a 10 ps time scale, and is dominated by non-radiative processes. In carotenoids having more than 9 conjugated double bonds, the fluorescence spectrum is often dominated by weak fluorescence from the  $S_2$  state, despite the fact that the  $S_2$  state has a subpicosecond lifetime. These characteristics indicate that carotenoid to chlorophyll energy transfer must be extremely rapid in order to be efficient. Recently, the energy gap law for non-radiative transitions has been used to relate the  $S_1$  energies obtained from the fluorescence spectra of a series of shorter carotenoids to their  $S_1$  lifetimes.<sup>1</sup> By using the empirical parameters from this relationship, reasonable estimates of the  $S_1$  energies of longer carotenoids with low  $S_1$  fluorescence yields can be made from measurements of their  $S_1$  lifetimes alone.<sup>1,7-11</sup> Energy transfer from the carotenoid  $S_2$  state may also be possible, as has been

suggested to occur in the light-harvesting antennas of purple bacteria,<sup>12</sup> but this must occur on a femtosecond time scale in order to be efficient.

The points raised above with regard to the difficulty of dealing with natural systems containing multiple chromophores suggest that studies employing simplified synthetic analogues of natural antenna systems may aid our understanding of natural systems. Model compounds consisting of covalently-linked carotenopyropheophorbide compounds have successfully demonstrated energy transfer from the carotenoid  $S_1$  to the pyropheophorbide  $S_1$  state.<sup>13-15</sup> In the present work we expand the scope of these studies by employing fucoxanthin and zeaxanthin energy donors, which possess  $S_1$  states that lie respectively above and below those of all five pyropheophorbide energy acceptors. Fucoxanthin in natural systems has been found to transfer energy to

(7) Frank, H. A.; Farhoosh, R.; Gebhard, R.; Lugtenburg, J.; Gosztola, D.; Wasielewski, M. R. *Chem. Phys. Lett.* **1993**, *207*, 88.

(8) Frank, H.; Cua, A.; Young, A.; Gosztola, D.; Wasielewski, M. R. *Photosynth. Res.* **1994**, *41*, 389.

(9) Frank, H. A.; Cua, A.; Chynwat, V.; Young, A.; Gosztola, D.; Wasielewski, M. R. *Biochim. Biophys. Acta* **1996**, *1277*, 243.

(10) Frank, H. A.; Desamero, R. Z. B.; Chynwat, V.; Gebhard, R.; van der Hoef, I.; Jansen, F. J.; Lugtenburg, J.; Gosztola, D.; Wasielewski, M. R. *J. Phys. Chem.* **1997**, *101*, 149.

(11) Chynwat, V.; Frank, H. A. *Chem. Phys.* **1995**, *194*, 237.

(12) Shreve, A. P.; Trautman, J. K.; Frank, H. A.; Owens, T. G.; Albrecht, A. C. *Biochem. Biophys. Acta* **1991**, *1058*, 280.

(13) Wasielewski, M. R.; Liddell, P. A.; Barrett, D.; Moore, T. A.; Gust, D. *Nature* **1986**, *322*, 570.

(14) Gust, D.; Moore, T. A.; Moore, A. L.; Devadoss, C.; Liddell, P. A.; Hermant, R.; Nieman, R. A.; Demanche, L. J.; DeGraziano, A. M.; Gouni, I. *J. Am. Chem. Soc.* **1992**, *114*, 3590.

(15) Osuka, A.; Shinoda, S.; Marumo, S.; Yamada, H.; Katoh, T.; Yamazaki, I.; Nishimura, Y.; Tanaka, Y.; Taniguchi, S.; Okada, T.; Nozaki, K.; Ohno, T. *Bull. Chem. Soc. Jpn.* **1995**, *68*, 3255.

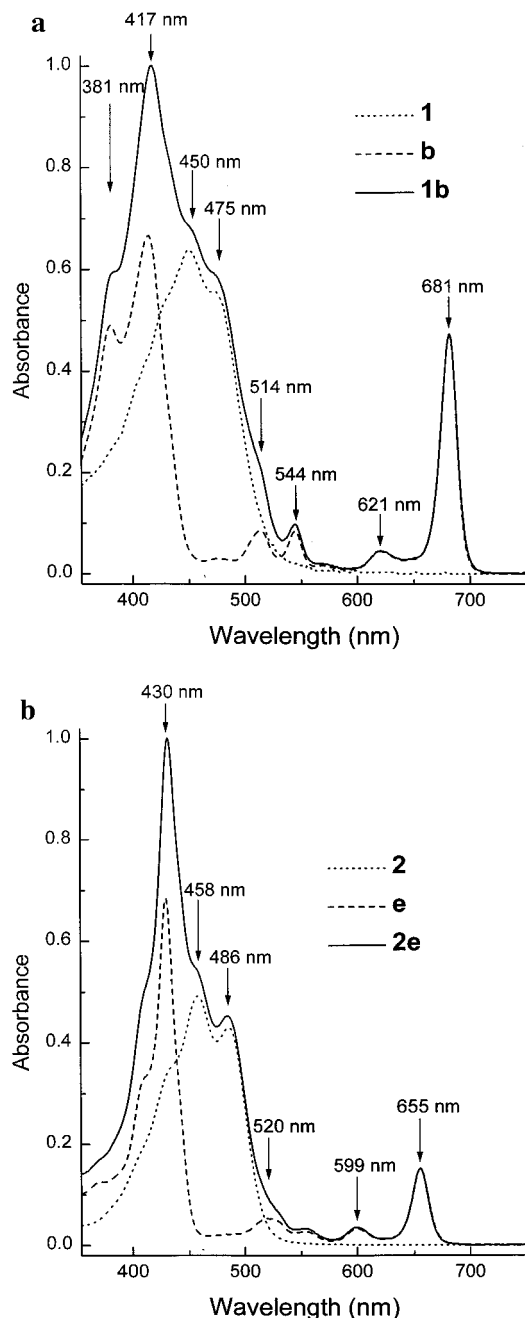


**Figure 2.** Ground-state absorption spectra of (a) molecules **1**, **b**, and **1b** in THF and (b) molecules **2**, **e**, and **2e** in THF.

chlorophyll *a* (Chl *a*) with high efficiency,<sup>16</sup> whereas zeaxanthin, a component of the xanthophyll cycle, is thought to be important as an excess energy quencher. Different pyropheophorbide derivatives were used to vary both the energy level of the  $S_1$  state of the acceptor and the degree of through-bond electronic coupling between the donor and acceptor, Figure 1. The transient absorption instrument used to measure the energy transfer rate constants produces a tunable excitation pulse and has better than 150 fs time resolution, allowing us to selectively excite the carotenoids and determine the extent of energy transfer from both the  $S_1$  and  $S_2$  states of the carotenoid to the pyropheophorbide.

## Results

Absorption spectra of reference molecules **1**, **2**, **b**, and **e** are compared with those of compounds **1b** and **2e** in Figure 2, parts

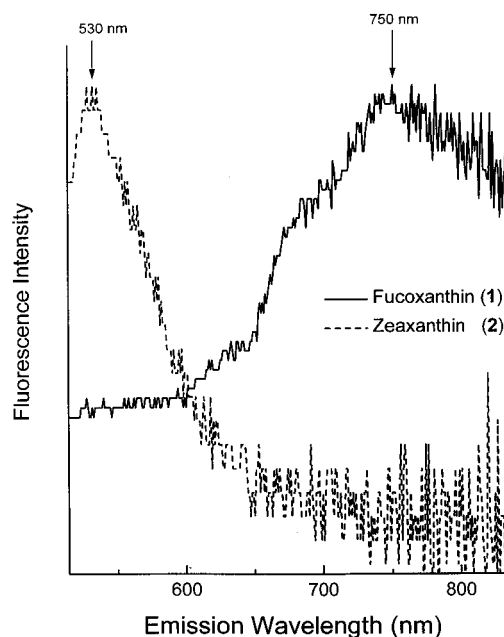


**Figure 3.** Steady-state emission spectra of **1** and **2** in THF. Excitation: 430 nm.

**Table 1.** Lowest Excited Singlet State Energies for Carotenoids and Pyropheophorbides

molecule	$S_1$ energy ( $\text{cm}^{-1}$ )	molecule	$S_1$ energy ( $\text{cm}^{-1}$ )
<b>1</b>	15 900	<b>c</b>	14 530
<b>2</b>	14 200	<b>d</b>	15 240
<b>a</b>	14 930	<b>e</b>	15 200
<b>b</b>	14 620		

a and b. For the transient absorption experiments, an excitation wavelength of 485 nm was chosen to maximize the ratio of carotenoid absorption to that of pyropheophorbide. Comparison of the absorption spectra of the carotenopyropheophorbide molecules with those of the carotenoids and pyropheophorbides alone shows that the absorption of the carotenoid is 10–25 times stronger than that of the pyropheophorbide at 485 nm. Fluorescence emission spectra of molecules **1** and **2** are shown in Figure 3. The short wavelength shoulder on the fucoxanthin spectrum has been suggested to be due to  $S_2$ -state emission, while the main peak at 750 nm is due to  $S_1$ -state emission.<sup>16</sup> However, it is possible that this band may be a vibronic band associated with the  $S_1$ -state emission. The zeaxanthin emission is from the  $S_2$  state exclusively.<sup>2</sup> The  $S_1$  energies of the pyropheophorbides were determined from the average of their  $Q_Y$  absorption and emission features, while those of fucoxanthin and zeaxanthin were estimated earlier.<sup>11,8</sup> These values are given in Table 1.

For each molecule, transient absorption kinetic data were recorded at 550 nm, near the peak of the carotenoid  $S_1 \rightarrow S_n$  excited state absorption, and 650–700 nm, at the peak of the ground-state absorption of the pyropheophorbide  $Q_Y$  band. Transient absorption spectra at several time delays were also recorded for each molecule. The transient absorption kinetics of molecules **1** and **1b** in THF, probed at 550 nm, are shown in Figure 4. The transient absorption signal for **1b**, reaching its peak in less than a picosecond, decays with two time constants of 37.9 ps and 6 ns. The slower time constant, accounting for only 5% of the decay amplitude, is due to the small population of excited pyropheophorbide molecules that are probed at this wavelength. The faster time constant corresponds to the  $S_1 \rightarrow S_0$  decay of the fucoxanthin. When compared with the kinetics of the fucoxanthin alone probed at 550 nm, which decays as a

(16) Shreve, A. P.; Trautman, J. K.; Owens, T. G.; Albrecht, A. C. *Chem. Phys.* **1991**, *154*, 171.

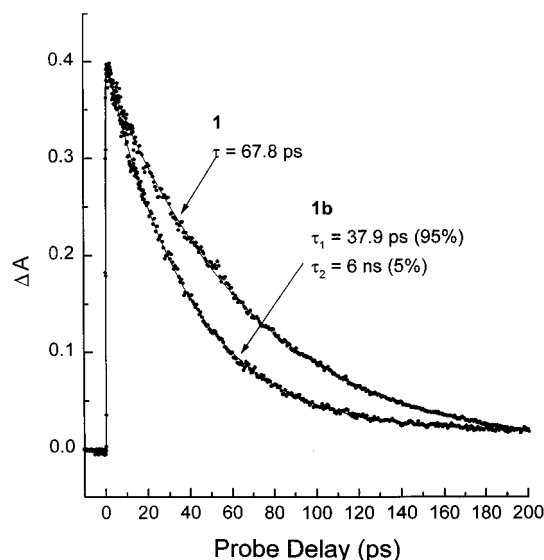


**Figure 4.** Transient absorption kinetics of molecules **1** and **1b** in THF excited at 485 nm and probed at 550 nm.

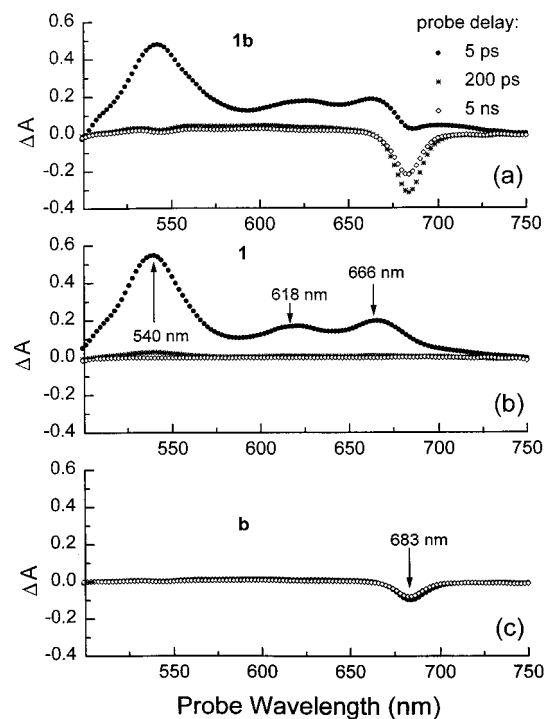


**Figure 5.** Transient absorption spectra of (a) **1**, (b) **b**, and (c) **1b** in THF excited at 485 nm.

single exponential with a 67.8 ps time constant, it is evident that linking pyropheophorbide to fucoxanthin has opened a new channel for decay of the  $S_1$  state of fucoxanthin. This new decay channel is singlet–singlet energy transfer from fucoxanthin to pyropheophorbide as evidenced by the transient absorption spectra of compounds **1b**, **1**, and **b** shown in Figure 5. At a probe delay of 5 ps, the spectrum of the linked fucoxanthin–pyropheophorbide, Figure 5a, closely resembles that of the excited state of fucoxanthin alone, Figure 5b, with only a small contribution from the excited state of the pyropheophorbide, Figure 5c. At a probe delay of 200 ps, the transient absorption spectrum of compound **1b** is mainly due to that of the pyropheophorbide  $S_1 \rightarrow S_n$  transition. The amplitude of the pyropheophorbide signal is clearly larger at 200 ps than at 5 ps, indicating that energy transfer has occurred from the fucoxanthin to the pyropheophorbide.

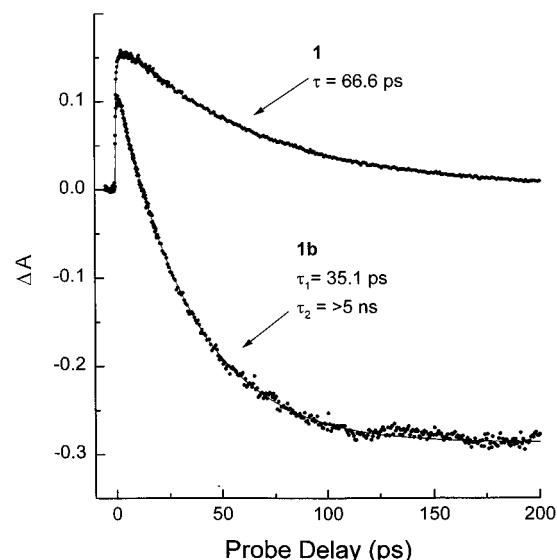


**Figure 6.** Transient absorption kinetics of molecules **1** and **1b** in THF excited at 485 nm and probed at 667 and 682 nm, respectively.

**Table 2.** Summary of the Decay Kinetics of Molecules **1**, **1a–e**, **2**, and **2a–e** Measured by Transient Absorption, Excited at 485 nm

probe wavelength (nm)	molecule	$\tau_{\text{decay}}$ (ps)	molecule	$\tau_{\text{decay}}$ (ps)
550	<b>1</b>	$67.8 \pm 0.5$	<b>2</b>	$9.1 \pm 0.1$
667		66.6		8.4
550	<b>1a</b>	58.0	<b>2a</b>	9.2
667		58.8		6.7
550	<b>1b</b>	37.9	<b>2b</b>	9.6
682		35.1		7.6
550	<b>1c</b>	40.3	<b>2c</b>	9.1
685		37.5		6.1
550	<b>1d</b>	52.5	<b>2d</b>	9.2
655		50.3		8.0
550	<b>1e</b>	60.0	<b>2e</b>	9.0
656		60.4		8.5

The transient absorption change for compound **1b**, monitored at 682 nm, Figure 6, is initially positive due to the contribution of the fucoxanthin excited state absorption. The signal then decays to a negative absorption with a 35.1 ps time constant, corresponding to the bleaching of the pyropheophorbide  $Q_Y$  band, in reasonable agreement with the 37.9 ps time constant for decay of the fucoxanthin excited state observed at 550 nm.

Assuming that covalent attachment of the pyropheophorbide onto the fucoxanthin does not affect the intrinsic lifetime of the lowest excited singlet state of fucoxanthin, the time constant for energy transfer from the fucoxanthin to the pyropheophorbide can be calculated according to:

$$\frac{1}{\tau_{\text{et}}} = \frac{1}{\tau_{\text{carot-chl}}} - \frac{1}{\tau_{\text{carot}}} \quad (1)$$

where  $\tau_{\text{carot-chl}}$  is the time constant for decay of **1b** probed at 550 nm,  $\tau_{\text{carot}}$  is the time constant for decay of fucoxanthin alone probed at 550 nm, and  $\tau_{\text{et}}$  is the time constant for energy transfer from the  $S_1$  state of fucoxanthin to the  $S_1$  state of pyropheophorbide. The result for compound **1b** is  $\tau_{\text{et}} = 86 \pm 2$  ps.

Time constants for energy transfer were calculated for the other pyropheophorbide–carotenoid compounds in a similar manner, Tables 2 and 3. For all molecules in which the carotenoid was fucoxanthin a time constant for energy transfer could be extracted, and the kinetics probed at 550 nm and at the peak of the pyropheophorbide  $S_1$  absorption (650–700 nm) were in reasonable agreement. In the case of the three fucoxanthin–pyropheophorbide compounds for which we mea-

**Table 3.** Time Constants for Energy Transfer from the Carotenoid  $S_1$  State to the Pyropheophorbide  $S_1$  State in Compounds **1a–e** and **2a–e**, Calculated from the Data in Table 2 by Using Eq 1

molecule	$\tau_{et}$ (ps)	$\Phi_{et}^a$ (%)	$\Phi_{et}^b$	molecule	$\tau_{et}$ (ps)	$\Phi_{et}^a$ (%)
<b>1a</b>	$400 \pm 50$	$14 \pm 2$	7	<b>2a</b>	$>600$	$<2$
<b>1b</b>	$86 \pm 2$	$44 \pm 1$	38	<b>2b</b>	<i>c</i>	<i>c</i>
<b>1c</b>	$99 \pm 6$	$41 \pm 3$	43	<b>2c</b>	$>300$	$<3$
<b>1d</b>	$230 \pm 20$	$23 \pm 2$	28	<b>2d</b>	$>850$	$<1$
<b>1e</b>	$520 \pm 80$	$12 \pm 2$	13	<b>2e</b>	$>200$	$<4$

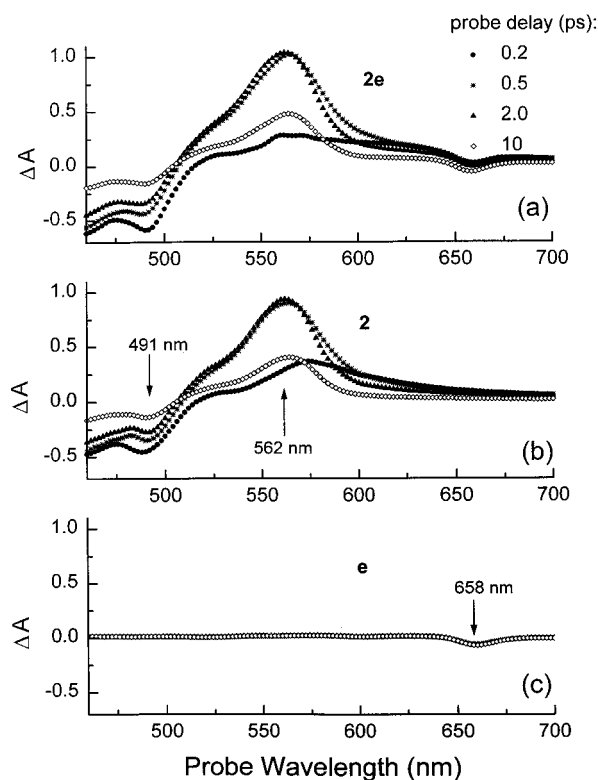
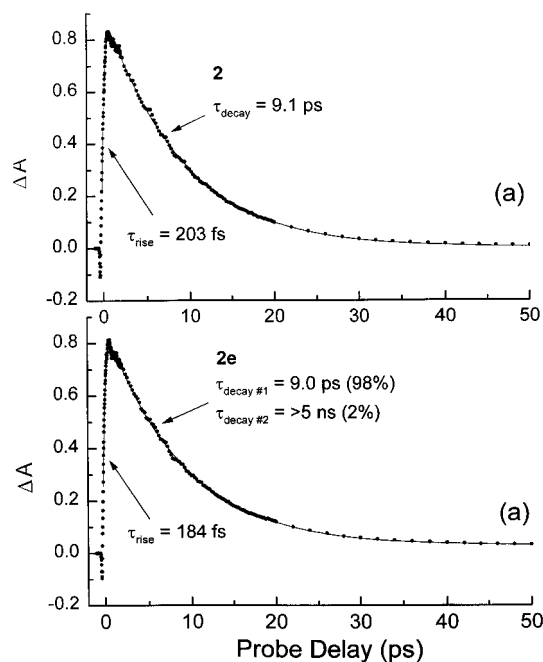
<sup>a</sup> Calculated from transient absorption kinetics according to eq 3.

<sup>b</sup> Obtained from steady-state fluorescence excitation spectra. <sup>c</sup> The decay time of **2b** is significantly longer than the decay time of **2**.

sured the fastest energy transfer times, **1b–d**, energy transfer from the carotenoid to the pyropheophorbide was clearly evident in the time progression of the transient absorption spectra, e.g. Figure 5a. In the case of zeaxanthin, however, none of the pyropheophorbide-linked compounds decayed significantly faster than zeaxanthin alone when probed at 550 nm. Thus, only upper limits for the rate constants for energy transfer from the carotenoid  $S_1$  state to the pyropheophorbide  $S_1$  state could be extracted. A further complication for each zeaxanthin-pyropheophorbide molecule is the fact that the time constant for the appearance of the pyropheophorbide absorption change (650–700 nm) is considerably faster than the time constant for decay of the zeaxanthin  $S_1 \rightarrow S_n$  absorption at 550 nm, see Table 2. This is the case even for zeaxanthin alone, **2**, when the kinetics probed at 550 and 667 nm are compared, and is likely due to the fact that the  $S_2 \rightarrow S_n$  transition of zeaxanthin is more intense in the 650–700-nm region than at 550 nm where the  $S_1 \rightarrow S_n$  transition dominates.

In an attempt to observe energy transfer from the  $S_2$  state of zeaxanthin to the  $S_1$  state of the covalently attached pyropheophorbide, transient absorption spectra were recorded at a series of early probe delay times: 0.2, 0.5, 2.0, and 10 ps, for all five zeaxanthin-pyropheophorbide compounds. The transient absorption spectra of zeaxanthin in THF are measured with high enough time resolution to capture excited-state absorption changes from both the  $S_2$  and  $S_1$  states. As an example, the transient absorption spectra of compound **2e** in THF are shown in Figure 7a. The positive absorption peak at 562 nm and the negative absorption peak at 658 nm are due respectively to the  $S_1 \rightarrow S_n$  absorption of zeaxanthin, Figure 7b, and the ground state bleaching of the pyropheophorbide, Figure 7c. At 0.2 ps, the transient absorption is broad with a tail extending well beyond 600 nm. At this time delay, a significant fraction of the excited zeaxanthin molecules are in the  $S_2$  state (*vide infra*). With increasing probe delay times the spectra shift toward the blue, perhaps corresponding to relaxation from the  $S_2$  state to the  $S_1$  state of zeaxanthin, with the maximum of the  $S_1 \rightarrow S_n$  transition occurring at  $\sim 562$  nm. The time evolution of the transient absorption spectra of **2e** in Figure 7a are difficult to distinguish from the summed contributions of the individually excited zeaxanthin and pyropheophorbide components. Similar results are observed for the four other zeaxanthin-pyropheophorbide compounds. In no case is there obvious evidence of excitation energy transfer from the zeaxanthin to the pyropheophorbide.

As a more sensitive test of the possibility of energy transfer from the carotenoid  $S_2$  state to the pyropheophorbide  $S_1$  state, the rise of the transient absorption signal at 550 nm was measured with a high density of probe delay time points for the zeaxanthin-containing molecules. Kinetic traces for molecules **2** and **2e** are compared in Figure 8, parts a and b, and the results for all of the zeaxanthin-containing compounds are summarized in Table 4. The rise times for compounds **2a–e**

**Figure 7.** Transient absorption spectra of (a) **2e**, (b) **2**, and (c) **e** in THF excited at 485 nm.**Figure 8.** Transient absorption kinetics of (a) **2** and (b) **2e** in THF excited at 485 nm and probed at 550 nm.

are all similar to that of molecule **2** but slightly shorter. The observed rise time of the transient absorption signal probed at 550 nm will depend on all processes that depopulate the  $S_2$  state of zeaxanthin. Thus, if energy transfer makes a significant contribution to the decay of the  $S_2$  state, the observed rise time ( $\tau_{rise}$ ) will be:

$$\frac{1}{\tau_{rise}} = \frac{1}{\tau_{IC}} + \frac{1}{\tau_F} + \frac{1}{\tau_{et}} \quad (2)$$

where  $\tau_{IC}$ ,  $\tau_F$ , and  $\tau_{et}$  are respectively the time constants for  $S_2$

**Table 4.** Summary of the Transient Absorption Rise Times ( $\tau_{\text{rise}}$ ) for Molecules **2** and **2a–e** Excited at 486 nm and Probed at 550 nm as Well as the Calculated Time Constants ( $\tau_{\text{et}}$ , Eq 2) and Quantum Yields ( $\Phi_{\text{et}}$ ) for Energy Transfer from the Carotenoid  $S_2$  State to the Pyropheophorbide  $S_1$  State

molecule	$\tau_{\text{rise}}$ (fs)	$\tau_{\text{et}}$ (ps)	$\Phi_{\text{et}}^a$	$\Phi_{\text{et}}^b$
<b>2</b>	203 ± 4			
<b>2a</b>	195	5 ± 3	4 ± 2%	2
<b>2b</b>	193	4 ± 2	5 ± 2%	8
<b>2c</b>	175	1.3 ± 0.2	13 ± 3%	11
<b>2d</b>	171	1.1 ± 0.2	15 ± 3%	15
<b>2e</b>	184	2.0 ± 0.5	9 ± 2%	12

<sup>a</sup> Calculated from transient absorption kinetics according to eq 3.<sup>b</sup> Obtained from steady-state fluorescence excitation spectra.

to  $S_1$  internal conversion within zeaxanthin, the radiative decay of the  $S_2$  state, and energy transfer from the zeaxanthin  $S_2$  state to the pyropheophorbide  $S_1$  state. Time constants for energy transfer from the carotenoid  $S_2$  state to the pyropheophorbide  $S_1$  state, calculated from eq 2, are summarized in Table 4. The calculated time constants for energy transfer are all much slower than the time constant for internal conversion and fluorescence so that the quantum yield for energy transfer is less than 20% in all cases. The quantum yields of energy transfer, also listed in Table 4, were calculated according to:

$$\Phi_{\text{et}} = \frac{k_{\text{et}}}{k_{\text{et}} + k_{\text{IC}} + k_{\Phi}} \quad (3)$$

These calculated quantum yields are in good agreement with quantum yields measured by steady-state fluorescence excitation.<sup>15</sup>

## Discussion

Previous studies<sup>13–15</sup> have suggested that electron exchange interactions<sup>17</sup> rather than Coulomb interactions<sup>18</sup> dominate the mechanism for energy transfer from carotenoids with short-lived  $S_1$  states linked to chlorophyll-like molecules with short tethers. The Coulomb mechanism was excluded on the basis of the forbidden nature of the  $S_1 \leftrightarrow S_0$  transition in many carotenoids, and the short ( $\sim 100$  fs) lifetime of the optically-allowed  $S_2 \leftrightarrow S_0$  transition.<sup>2</sup> More recently, however, it has been noted that even carotenoids with zero  $S_1 \leftrightarrow S_0$  transition dipole oscillator strength can undergo energy transfer by the Coulomb mechanism once multipole interactions are included in the rate expressions.<sup>19</sup> In addition, in carotenoids such as fucoxanthin, whose symmetry is broken, the  $S_1$  state may “borrow” oscillator strength from the  $S_2$  state, making dipole–dipole interactions non-zero as well.<sup>16</sup> Extremely rapid energy transfer from the carotenoid  $S_2$  state has also been suggested to occur in photosynthetic antenna proteins.<sup>12</sup>

In the present studies, a minimum of 7 saturated bonds separate the  $\pi$  systems of the fucoxanthin and pyropheophorbide molecules. Since through-bond electron exchange interactions decrease exponentially with distance,<sup>13</sup> it is not likely that the Dexter mechanism significantly contributes to the overall efficiency of fucoxanthin  $S_1$  to pyropheophorbide  $S_1$  energy transfer. There is no evidence from ring current shifts in the <sup>1</sup>H NMR spectra of the fucoxanthin–pyropheophorbide molecules that these molecules adopt conformations in which the fucoxanthin folds over the pyropheophorbide. Therefore, the direct orbital overlap necessary for a significant contribution by the Dexter mechanism is minimal. This fact combined with

**Table 5.** Factors Used in Calculations of the Time Constant ( $\tau_{\text{et}}$ ) for Energy Transfer from Carotenoid to Pyropheophorbide<sup>a</sup>

molecule	$R_{\text{DA}}$ (Å)	$\kappa^2$ <sup>b</sup>	$\kappa^2$ <sup>c</sup>	$V^2$ (cm <sup>-6</sup> , × 10 <sup>40</sup> )	$\epsilon$ (M <sup>-1</sup> cm <sup>-1</sup> , × 10 <sup>-4</sup> )	$I$ (cm <sup>6</sup> mol <sup>-1</sup> , × 10 <sup>11</sup> )
<b>1a</b>	22.9	0.28	0.02	0.016	5.43 (668 nm)	9.3
<b>1b</b>	18.5	1.16	0.92	6.3	6.20 (682 nm)	12.6
<b>1c</b>	18.5	1.00	0.85	6.1	5.49 (685 nm)	14.2
<b>1d</b>	18.5	1.18	0.93	6.3	4.42 (655 nm)	5.4
<b>1e</b>	21.0	0.09	0.09	8.0	3.58 (655 nm)	5.1
<b>2a</b>	21.1	3.43	3.26	6.6		5.1
<b>2b</b>	20.1	1.49	1.65	4.4		4.1
<b>2c</b>	20.2	1.49	1.69	4.6		4.1
<b>2d</b>	20.3	1.52	1.66	4.4		3.6
<b>2e</b>	21.2	3.53	3.39	5.7		5.0

<sup>a</sup>  $R_{\text{DA}}$ : center-to-center separation distance.  $\kappa$ : dipole–dipole orientation term.  $V$ : transition monopole interaction energy.  $\epsilon$ : molar decadic extinction coefficient.  $I$ : integral for overlap of carotenoid fluorescence with pyropheophorbide absorbance. <sup>b</sup> Calculated using transition dipoles. Pyropheophorbide transition dipoles were calculated from positions of opposing pyrrole nitrogens. Carotenoid transition dipoles were calculated from positions of carbons on the ends of the conjugated path (Figure 1: atoms  $x$  and  $y$  on compounds **1** and **2**). <sup>c</sup> Calculated using transition dipoles. Pyropheophorbide transition dipoles were calculated by using the published wave functions for bacteriopheophytin b.<sup>21</sup> Fucoxanthin and zeaxanthin transition dipoles calculated from  $S_2$  transition monopoles published for neurosporene.<sup>19</sup>

**Table 6.** Comparison of Calculated and Measured Time Constants ( $\tau_{\text{et}}$ ) for Energy Transfer from Carotenoid to Pyropheophorbide

molecule	transition	$\tau_{\text{et}}^{\text{exp}}$ (ps)	$\tau_{\text{et}}^{\text{calc } a}$ (ps)	$\tau_{\text{et}}^{\text{calc } b}$ (ps)	$\tau_{\text{et}}^{\text{calc } c}$ (ps)
<b>1a</b>	$S_1 \rightarrow Q_Y$	400	2500	29000	30000
<b>1b</b>	$S_1 \rightarrow Q_Y$	86	120	150	56
<b>1c</b>	$S_1 \rightarrow Q_Y$	99	120	150	52
<b>1d</b>	$S_1 \rightarrow Q_Y$	230	280	360	130
<b>1e</b>	$S_1 \rightarrow Q_Y$	520	8200	7900	1080
<b>2a</b>	$S_2 \rightarrow Q_X$	5	8.4	8.8	4.9
<b>2b</b>	$S_2 \rightarrow Q_X$	4	14	13	7.5
<b>2c</b>	$S_2 \rightarrow Q_X$	1.3	12	11	5.7
<b>2d</b>	$S_2 \rightarrow Q_X$	1.1	17	16	8.3
<b>2e</b>	$S_2 \rightarrow Q_X$	2.0	7.0	7.3	4.8

<sup>a</sup> Calculated with transition dipoles. Pyropheophorbide transition dipoles were calculated from positions of opposing pyrrole nitrogens. Carotenoid transition dipoles calculated from positions of carbons on the ends of the conjugated path (Figure 1: atoms  $x$  and  $y$  on compounds **1** and **2**). <sup>b</sup> Calculated with transition dipoles. Pyropheophorbide transition dipoles calculated by using the published wave functions for bacteriopheophytin b.<sup>21</sup> Fucoxanthin and zeaxanthin transition dipoles calculated from  $S_2$  transition monopoles published for neurosporene.<sup>19</sup> <sup>c</sup> Calculated with transition monopoles, uncorrected.

the fact that the  $S_1 \leftrightarrow S_0$  transition in fucoxanthin is weakly allowed make the Coulomb (Förster) mechanism a stronger candidate for the mechanism of singlet–singlet energy transfer in the fucoxanthin–pyropheophorbide case than the electron exchange (Dexter) mechanism. The strongly allowed nature of the  $S_2 \leftrightarrow S_0$  transition in the zeaxanthin-containing compounds makes it likely that the Förster mechanism will contribute to energy transfer from the zeaxanthin  $S_2$  state as well, despite the fact that the lifetime of the zeaxanthin  $S_2$  state is only 200 fs. Calculations of the rate constants for energy transfer from the carotenoid to the pyropheophorbide in molecules **1a–e** and **2a–e**, based on the Förster model in the weak coupling limit, are summarized in Tables 5 and 6. The Förster model predicts that the rate constant for energy transfer is proportional to the spectral overlap of the fluorescence of the donor with the absorbance of the acceptor (see eq 4 in the Experimental Section). The steady-state fluorescence spectrum of fucoxanthin, originating from the  $S_1$  state, peaks at 750 nm, Figure 3, and overlaps most strongly with the pyropheophorbide  $Q_Y$  absorption bands. The steady-state fluorescence spectrum

(17) Dexter, D. L. *J. Chem. Phys.* **1953**, *21*, 836.(18) Förster, T. In *Modern Quantum Chemistry*; Sinanoglu, O., Ed.; Academic Press: New York, 1965; Vol. 3, pp 93–137.(19) Nagae, H.; Kakitani, T.; Mimuro, M. *J. Chem. Phys.* **1993**, *98*, 8012.

of zeaxanthin, originating from the  $S_2$  state, peaks at 530 nm, Figure 3, and overlaps most strongly with the  $Q_X$  region of the pyropheophorbide absorption spectrum. Thus, the calculations performed for molecules **1a–e** use the transition dipole/monopoles of the pyropheophorbide  $Q_Y$  state as the acceptor state, and it is assumed that energy is being transferred from the fucoxanthin  $S_1$  state. For molecules **2a–e** the calculations employ the pyropheophorbide  $Q_X$  state, and it is assumed that energy is being transferred from the zeaxanthin  $S_2$  state. The partially allowed  $S_1 \leftrightarrow S_0$  transition in fucoxanthin is assumed to be in the same direction as the strongly allowed  $S_2 \leftrightarrow S_0$  transition.

The Förster calculations were performed at three levels. At the simplest level, the donor and acceptor transitions were treated as point dipoles. The minimum energy conformations of the carotenoid-pyropheophorbide compounds were estimated by molecular mechanics calculations.<sup>20</sup> The center and orientation of the transition dipoles of the pyropheophorbide  $Q_X$  and  $Q_Y$  bands were estimated by using the positions of the opposing nitrogens in the pyropheophorbide ring: rings 1 and 3 for  $Q_Y$  and rings 2 and 4 for  $Q_X$ . The orientation of the transition dipoles of the carotenoids was estimated by using the positions of the carbon atoms near the ends of the conjugated paths: atoms  $x$  and  $y$  on molecules **1** and **2** in Figure 1. The centers of the transition dipoles of the carotenoids were estimated by using the positions of the carbon atoms near the center of the conjugated paths, atoms  $q$  and  $r$  on molecules **1** and **2** in Figure 1. At the second level of calculation, the transition dipole directions for the pyropheophorbides were taken as the values calculated for bacteriopheophytin *b* by Warshel and Parson,<sup>21</sup> while the transition dipole directions for the carotenoids were taken as the values calculated for neurosporene, a carotenoid containing 9 conjugated double bonds.<sup>19</sup> The results of these first two levels of calculation are in reasonable agreement with each other, see Table 6, except in the case of compound **1a**, where the long axis of the fucoxanthin and the pyropheophorbide  $Q_Y$  transitions are nearly perpendicular. At the third level of calculation, the dipole-dipole calculations were extended to multipole calculations by treating the transitions as point monopoles located on the individual atoms of the donors and acceptors. The transition monopoles were again taken as those of bacteriopheophytin *b*<sup>21</sup> and neurosporene.<sup>19</sup>

The point dipole calculations underestimate the strength of the Coulomb interaction between the carotenoid and pyropheophorbide transitions. The multipole method overestimates the rate constants for energy transfer in the fucoxanthin-containing molecules and underestimates the rate constants for energy transfer in the zeaxanthin-containing molecules. This may be attributable to the choice of neurosporene as a reference for the transition monopoles. Neurosporene, containing 9 carbon double bonds in its conjugated path, is longer than the conjugation path of fucoxanthin (8 conjugated double bonds) but shorter than that of zeaxanthin (11 conjugated double bonds).

The Förster calculations are in best agreement with experimental measurements in the cases of the three fucoxanthin-containing molecules **1b–d**. The calculations suggest that there are several reasons why these particular compounds show rapid energy transfer from the fucoxanthin to the pyropheophorbide: First, the attachment of the fucoxanthin onto the pyropheophorbide at  $C_2$  on ring 1 results in a shorter center-to-center distance (18.5 Å) between the chromophore transition dipoles as compared to attachment at  $C_1$  on ring 2 (compound **1e**, 21.0 Å)

or attachment at the end of the propionic side chain of ring 4 (compound **1a**, 22.9 Å). Second, the point of attachment in compounds **1b–d** also results in a more favorable orientation ( $\kappa^2$ , Table 5) of the donor and acceptor transition dipoles for energy transfer than in compounds **1a** and **1e**, especially in compound **1e**, which possesses a more flexible linkage between the donor and acceptor. The flexible linkage between the fucoxanthin and pyropheophorbide will lead to the largest uncertainties in relative chromophore position and orientation when the distance between the chromophores is greatest, as in compound **1a**, and when the time scale for energy transfer is comparable to or longer than the time scale for conformational motion. Third, the overlap ( $I$ , Table 5) of the  $S_1$  fluorescence of the fucoxanthin with the  $Q_Y$  absorption of the pyropheophorbide is strong, particularly for compounds **1b** and **1c**.

The predicted time constants for energy transfer in the zeaxanthin-containing compounds **2a–e** are in much poorer agreement with the observed time constants than is the case for the fucoxanthin-containing compounds (**1a–e**). The predicted time constants for compounds **2a–e** are considerably slower than the measured values. In addition to the disagreement in magnitude, the predicted and observed trends are also uncorrelated: the slowest observed time constant of the five compounds is the second fastest in the Förster calculations, whereas the fastest observed time constant is the second slowest in the Förster calculations. The disagreement between the energy transfer time constants in molecules **2a–e** predicted by the Förster calculations and observed experimentally is probably not due to experimental inaccuracy: the observed quantum yields for energy transfer as measured by two different methods, transient absorption and steady-state fluorescence, are in close agreement. Instead, the error apparently lies in the energy transfer model. Besides the error involved in approximating the transition monopoles of zeaxanthin and the pyropheophorbides, a likely source of error in the Förster calculations is in the overlap integral (eq 4). The Förster model assumes that following excitation, the donor state relaxes vibrationally before energy transfer takes place. This is likely to be the case for the  $S_1$  state of the fucoxanthin from which energy is transferred, but in zeaxanthin in which rapid energy transfer is occurring from the short-lived  $S_2$  state, it is unlikely that complete vibrational equilibration is achieved. In the fucoxanthin-containing series the minimum number of saturated bonds between the  $\pi$  systems is 7 for molecules **1b–e**, whereas the minimum number falls to 4 in the corresponding zeaxanthin series, **2b–e**. Since the through-bond electronic coupling between the energy donor and acceptor depends on the number of saturated bonds connecting them, it is possible that through-bond energy transfer,<sup>17</sup> i.e. the Dexter mechanism, contributes more significantly to energy transfer from zeaxanthin to pyropheophorbide than from fucoxanthin to pyropheophorbide.

## Conclusions

Experimentally observed singlet-singlet energy transfer rate constants for the fucoxanthin-pyropheophorbide compounds are consistent with calculated rate constants for energy transfer based on the Coulomb interaction between the fucoxanthin and pyropheophorbide singlet transitions. The partially allowed nature of the fucoxanthin  $S_1$  transition combined with the multiple saturated bonds separating the fucoxanthin and pyropheophorbide molecules appears to make the Coulomb mechanism more favorable than the electron exchange mechanism.

On the other hand, energy transfer from the  $S_1$  state of zeaxanthin to that of pyropheophorbide is very inefficient in

(20) The molecular mechanics calculations were performed with use of a modified MM2 model with Hyperchem (Hypercube, Waterloo, Ontario).

(21) Warshel, A.; Parson, W. W. *J. Am. Chem. Soc.* **1987**, *109*, 6143.

all the zeaxanthin–pyropheophorbide compounds examined. This is most likely due to the fact that the zeaxanthin  $S_1$  state energy is below that of all five pyropheophorbides investigated here. In addition, for molecules **2b** and **2c**, which are most likely to have zeaxanthin  $S_1$  energies close to that of the pyropheophorbide, the short 9.1-ps lifetime of the zeaxanthin  $S_1$  state and the formally forbidden nature of the zeaxanthin  $S_1$  to  $S_0$  optical transition also contribute to the lack of  $S_1$  to  $S_1$  energy transfer efficiency. Energy transfer efficiency from the zeaxanthin  $S_2$  state in molecules **2a–e** is as high as 15%. The  $S_2$  energy level overlaps well with the  $Q_X$  region of the pyropheophorbide absorption spectrum, and the  $S_2$  to  $S_0$  transition is allowed. These results in combination with our previous results on carotenoid–pyropheophorbide energy transfer<sup>13</sup> suggest that a wide spectrum of energy transfer mechanisms is available to carotenoids to optimize the efficiency of energy transfer to chlorophylls. Further work is necessary to determine how each of these mechanisms depends on the details of carotenoid and chlorophyll structure within proteins.

## Experimental Section

Tetrahydrofuran was refluxed over  $\text{LiAlH}_4$ , distilled, stored under nitrogen, and used within 2 days after distillation. A description of the synthesis of the carotenoid–pyropheophorbide compounds used in this study has already appeared.<sup>22</sup>

**Photophysical Measurements.** Ground state absorption measurements were made on a Shimadzu spectrometer (UV160). Fluorescence emission and excitation spectra were taken on a Shimadzu RF-5300PC spectrofluorophotometer specially equipped with a Hamamatsu R928 photomultiplier to measure corrected fluorescence spectra up to 900 nm. Zeaxanthin was a gift from Roche Japan Co. (Tokyo) and was used without purification. Fucoxanthin was extracted from thali of the brown alga *Dilophus okamurai* and purified by repeated flash column chromatography over silica gel and reverse phase column chromatography over Cosmosil75 C18-OPN (Nacalai Tesque). The purity of these carotenoids was checked by fluorescence emission spectroscopy, and they exhibit properties identical with those reported by Mimuro et al.<sup>23</sup> The fluorescence quantum yields of fucoxanthin (**1**) and zeaxanthin (**2**) in THF at room temperature were measured, by comparison with a standard (fluorescein in 0.1 M NaOH,  $\Phi = 0.90$ ),<sup>24</sup> to be  $6.8 \times 10^{-4}$  and  $6.6 \times 10^{-5}$ , respectively. Corrected fluorescence emission spectra were limited to wavelengths less than 900 nm, making it necessary to estimate the long wavelength tail of the fucoxanthin spectrum by Gaussian extrapolation. The extinction coefficients of each compound were determined by dissolving about  $0.3 \text{ mg} \pm 0.1 \text{ } \mu\text{g}$  in 25 mL of THF. This solution was diluted to 125 mL. The absorption spectra of these solutions were determined on the Shimadzu UV-2400PC. Each determination was performed twice with good reproducibility.

Transient absorption experiments were performed on samples dissolved in THF at room temperature in a 1 or 2 mm path length cell. For the transient absorption experiments the 412–420-nm pulses obtained by frequency doubling a regeneratively-amplified Ti:sapphire laser<sup>25</sup> were used to pump an optical parametric amplifier that furnishes

150-fs transform-limited pulses that are tunable from 470 to 820 nm with energies up to  $5 \text{ } \mu\text{J}$  per pulse at a 1.3 kHz repetition rate.<sup>26</sup> Typical pulse energies used to excite the molecules used in this study were about  $1 \text{ } \mu\text{J}$ /pulse at 485 nm with a beam waist of  $300 \text{ } \mu\text{m}$  inside the sample. Transient absorption spectra were recorded between 450 and 800 nm with a 2 nm step size, and the monochromator set to a bandwidth of 4 nm. The different colors in the white light probe pulse were compensated to arrive at the sample at the same time, within 150 fs. This was achieved by active delay compensation at each probe wavelength chosen by the monochromator. Kinetic data were recorded with variable probe delay step sizes so that a higher density of points was recorded at the earliest times following the pump pulse. The probe delay was limited to 5 ns.

**Förster Calculations.** Calculations of the rate constants for energy transfer from carotenoid to pyropheophorbide were performed by using Förster's model in the weak coupling limit:<sup>18</sup>

$$k_{\text{DA}} = \frac{9 \ln 10}{128\pi^5 N_A n^4 R_{\text{DA}}^6} \frac{\Phi_{\text{D}} \epsilon_{\text{A}}}{\tau_{\text{D}}} \int_0^{\infty} F_{\text{D}}(\lambda) A_{\text{A}}(\lambda) \lambda^4 d\lambda \quad (4)$$

$$\kappa = \hat{\mu}_{\text{D}} \cdot \hat{\mu}_{\text{A}} - 3(\hat{\mu}_{\text{D}} \cdot \hat{r}_{\text{DA}})(\hat{\mu}_{\text{A}} \cdot \hat{r}_{\text{DA}}) \quad (5)$$

where  $n$ , the index of refraction, is 1.41 for THF at room temperature,  $N_A$  is Avogadro's number,  $R_{\text{DA}}$  is the distance (in cm) separating the centers of the transition dipoles of the donor (carotenoid) and acceptor (pyropheophorbide),  $\Phi_{\text{D}}$  and  $\tau_{\text{D}}$  are the fluorescence quantum yield and lifetime (in s) of the donor,  $\epsilon_{\text{A}}$  is the extinction coefficient of the acceptor (in  $\text{cm}^2 \text{ mol}^{-1}$ ),  $F_{\text{D}}$  is the fluorescence spectrum of the donor normalized to integrate to 1,  $A_{\text{A}}$  is the absorption of the acceptor normalized to peak at 1,  $\lambda$  is the wavelength (in cm), and  $\kappa_{\text{DA}}$  depends on the relative orientation of the unit vectors describing the direction of the chromophore transition dipole moments ( $\hat{\mu}_{\text{D}}$  and  $\hat{\mu}_{\text{A}}$  for donor and acceptor, respectively) and their orientation relative to the unit vector separating their centers ( $\hat{r}_{\text{DA}}$ ) as shown in eq 5.

The above model treating transitions as point dipoles can be expanded to include multipole interactions by treating atoms on the donor and acceptor as point monopoles. This is accomplished by replacing  $\kappa^2/R_{\text{DA}}^6$  in eq 4 with:

$$\frac{V^2}{|\mu_{\text{D}}|^2 |\mu_{\text{A}}|^2} = \frac{1}{|\mu_{\text{D}}|^2 |\mu_{\text{A}}|^2} \left( \sum_{i,j} \frac{\rho_i \rho_j}{R_{ij}} \right)^2 \quad (6)$$

where  $V$  is the Coulomb interaction energy between the transition monopoles on the donor ( $\rho_i$ ) and acceptor ( $\rho_j$ ), and  $R_{ij}$  is the distance between atoms  $i$  and  $j$ . The transition monopoles are related to the transition dipole according to:

$$\vec{\mu}_i = \sum_j \rho_j r_j \quad (7)$$

where  $r_i$  describes the position of atom  $i$ .

**Acknowledgment.** Work at Argonne and Northwestern University was supported by the Division of Chemical Sciences, Office of Basic Energy Sciences, United States Department of Energy under contract No. W-31-109-Eng-38. Work at Kyoto University was supported by a Grant-in-Aid for Scientific Research (No. 08874074) from the ministry of Education, Science, Sports, and Culture of Japan and the Asahi Glass Science Foundation.

JA970594E

(22) Shinoda, S.; Osuka, A.; Nishimura, Y.; Yamazaki, I. *Chem. Lett.* **1995**, 1139.

(23) Mimuro, M.; Nishimura, Y.; Takaichi, S.; Yamano, Y.; Ito, M.; Nagaoka, S.; Yamazaki, I.; Katoh, T.; Nagashima, U. *Chem. Phys. Lett.* **1993**, 213, 576.

(24) Demas, J. N.; Crosby, G. A. *J. Phys. Chem.* **1971**, 75, 991.

(25) Gosztoła, D.; Yamada, H.; Wasielewski, M. R. *J. Am. Chem. Soc.* **1995**, 117, 2041.

(26) Greenfield, S. R.; Wasielewski, M. R. *Opt. Lett.* **1995**, 20, 1394.